Inorg. Chem. **2008**, *47*, 1261−1263

Low-Temperature Approach to Synthesize Iron Nitride from Amorphous Iron

Yi Han,[†] Huamin Wang,[†] Minghui Zhang,[*,†] Ming Su,[‡] Wei Li,[†] and Keyi Tao[†]

Institute of New Catalytic Materials Science, College of Chemistry, Nankai University, Tianjin 300071, and China and NanoScience Technology Center, Department of Mechanical, Materials, Aerospace Engineering, University of Central Florida, Orlando, Florida 32826

Received June 12, 2007

Iron nitride was prepared by a nitridation reaction in NH_3 using amorphous iron as precursor. The precursor was prepared at ambient temperature through the process of reducing ferrous sulfate by potassium borohydride, followed by the nitridation at different temperatures. The nitridation reaction occurred at 548 K, and ϵ-$Fe_{2-3}N$ was formed at 573 K. The reaction temperature was much lower than that using crystallized iron because of the characteristics of the amorphous materials. The existence of a small quantity of boron (1.6 wt.%) improved the stability of the amorphous precursor, which guaranteed an amorphous iron precursor at nitriding temperatures in excess of 548 K.

Transition metal nitrides have attracted great attention in recent years because of their unique physical and chemical characteristics, including outstanding optical, electrical, magnetic, and mechanical properties.[1−3] In particular, iron nitrides have been widely used as magnetic, optical recording materials and catalysts.[4−7] The most frequently used method for the synthesis of iron nitride is the thermal ammonolysis reaction. The iron powders are treated in the NH_3 flow to obtain iron nitride, and the temperature must be at 773 K or even higher.[8] With an increase of reaction temperature, iron first undergoes initial nitriding to Fe_4N, and then a further nitridation occurs to form $Fe_{2-3}N$ (or Fe_3N_{1+x}) and Fe_2N. Other methods in the formation of iron nitride have also been reported, such as reactive magnetron sputtering, plasma nitriding, ball milling, chemical vapor deposition (CVD), ion implantation, laser nitriding, ion beam assisted evaporation, solid-state metathesis, etc.[4,9−17] In general, the high temperature required in the nitridation process incorporates a negative effect upon the properties of iron nitrides. A low-temperature route to the synthesis of these nitrides is currently of considerable interest. K. Lu et al.[18,19] demonstrated that, when the surface of an elemental iron plate (7 mm by 100 mm by 100 mm in size) was refined to the nanometer scale by a surface mechanical attrition treatment, the iron plate could be nitrided at a temperature as low as 573 K. As demonstrated in their work, the nanostructures have a high density of nonequilibrium defects and store an excess Gibbs free energy in the grain boundaries. The excess energies provide extra driving force for nitride formation.

In this respect, amorphous material, which possesses a highly disordered structure and a large number of defects, can store abundant excess free energy to facilitate the reaction occurring at lower temperature.[20,21] In terms of the nitridation of iron, it is proposed that, with amorphous iron used as the

* To whom correspondence should be addressed. E-mail: zhangmh@nankai.edu.cn. Phone/Fax: +86-22-23507730

[†] Nankai University.

[‡] University of Central Florida.

(1) Toth, L. E., *Transition Metal Carbides and Nitrides*, Academic Press: New York, 1971.
(2) Oyama, S. T. *The Chemistry of Transition Metal Carbides and Nitrides*; Blackie Academic Professional: Glasgow, 1996.
(3) Eck, B.; Dronskowski, R.; Takahashib, M.; Kikkawa, S. *J. Mater. Chem.* **1999**, *9*, 1527.
(4) Schaaf, P. *Prog. Mater. Sci.* **2002**, *47*, 1.
(5) Seiichi, A.; Masahiro, K. *Appl. Phys. Lett.* **1985**, *46*, 792.
(6) Ortiz, C.; Dumpich, G.; Morrish, A. H *Appl. Phys. Lett.* **1994**, *65*, 2737.
(7) Loloee, R.; Nikolaev, K. R.; Pratt, W. P. *Appl. Phys. Lett.* **2003**, *82*, 3281.
(8) Jacobs, H.; Rechenbach, D.; Zachwieja, U. *J. Alloys Compd.* **1995**, *227*, 10.
(9) Wang, X.; Zheng, W. T.; Tian, H. W.; Yu, S. S.; Xu, W.; Meng, S. H.; He, X. D.; Han, J. C.; Sun, C. Q.; Tay, B. K. *Appl. Surf. Sci.* **2003**, *22*, 30.
(10) Jirásková, Y.; Havlícek, S.; Schneeweiss, O.; Perina, V.; Blawert, C *J. Magn. Magn. Mater.* **2001**, *234*, 477.
(11) Chen, Y.; Halstead, T.; Williams, J. S. *Mater. Sci. Eng. A: Struct. Mater. Prop. Microstruct. Process.* **1996**, *206*, 24.
(12) Roberson, S. L.; Finello, D.; Banks, A. D.; Davis, R. F. *Thin Solid Films* **1998**, *326*, 47.
(13) Lu, Y. F.; He, Z. F.; Mai, Z. H.; Ren, Z. M. *J. Appl. Phys.* **2002**, *88*, 7095.
(14) Chatbi, H.; Vergnat, M.; Bauer, Ph.; Marchal, G. *Appl. Phys. Lett.* **1995**, *67*, 430.
(15) Zhao, H. Z.; Lei, M.; Chen, X. L.; Tang, W. H. *J. Mater. Chem.* **2006**, *16*, 4407.
(16) Shih, K. K.; Re, M. E.; Dove, D. B. *Appl. Phys. Lett.* **1990**, *57*, 412.
(17) Nakajima, K.; Okamoto, S. *Appl. Phys. Lett.* **1989**, *54*, 2536.
(18) Tong, W. P.; Tao, N. R.; Wang, Z. B.; Lu, J.; Lu, K. *Science* **2003**, *299*, 686.
(19) Tong, W. P.; Tao, N. R.; Wang, Z. B.; Zhang, H. W.; Lu, J.; Lu, K. *Scr. Mater.* **2004**, *50*, 647.
(20) Akihisa I.; Hashimoto K. *Amorphous and Nanocrystalline Materials: Preparation, Properties and Application*; Springer: Berlin, 2001; Vol. *6*, No. 4.
(21) Popescu, M. A. *Non-Crystalline Chalcogenides*; Kluwer Academic Publishers: Dordrecht, The Netherlands, 2000.

10.1021/ic702171s CCC: $40.75
Published on Web 01/17/2008

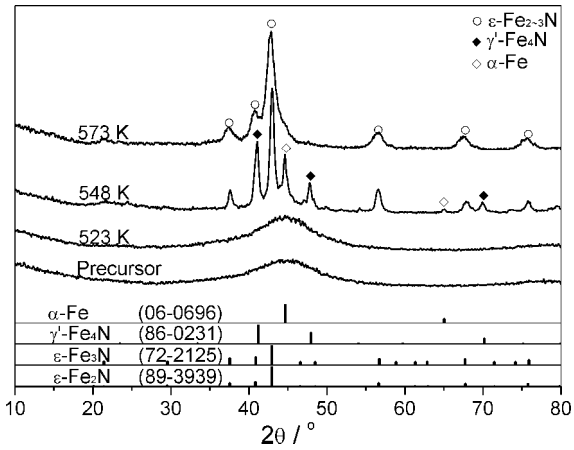

Figure 1. XRD pattern of the precursor and products nitrided at different temperatures.

precursor, the extra driving force stored in the metastable structure promotes the nitridation to occur at lower temperature. Therefore, we proposed a new route to prepare iron nitride from an amorphous iron precursor. The precursor was obtained through the reduction of ferrous sulfate by potassium borohydride. The nitridation occurred at a low temperature of 548 K, and ϵ-$Fe_{2-3}N$ was synthesized at 573 K, which was the lowest nitriding temperature by thermal ammonolysis method up to now.

The amorphous iron precursor was prepared by the chemical reduction at ambient temperature. An aqueous solution of potassium borohydride (1.0 mol/L) was added slowly to a 0.05 mol/L ferrous sulfate aqueous solution under vigorous stirring. The molar ratio of BH_4^-/Fe^{2+} was 3:1, and the temperature was 298 K. The reaction system was protected by argon atmosphere to avoid oxidation of products. The resulting amorphous iron was washed thoroughly with distilled water and anhydrous ethanol in sequence.

The fresh amorphous iron precursor (2.0 g) was placed in a quartz tube immediately, and dried in a flow of argon (20 mL/min) at 333 K. Then the precursor was heated in NH_3 flow (60 mL/min) at a rate of 10 K min^{-1} until it reached a certain temperature. After it was held at this temperature for 10 h, the sample was cooled to ambient temperature under a flow of NH_3 and then was treated in a flow of argon for several hours at ambient temperature to remove the nitrogen and hydrogen adsorbed on the surface.

As shown in Figure 1, the peak in the X-Ray diffraction (XRD) pattern of the amorphous iron precursor is diffused. The transmission electron microscopy (TEM) image in Figure 2a shows that the spherical amorphous iron aggregates into the chains. High-resolution transmission electron microscope (HRTEM) image (Figure 2b) shows that the precursor lacks long-range order, namely, the crystal lattice is not found in the inner region. In addition, the selected area electron diffraction (SAED) pattern (inset of Figure 2b) shows a diffuse halo, which confirms that the precursor is amorphous. Energy dispersive X-ray spectrometry (EDX) result shows that there is mainly Fe (98.4 wt %) with a small quantity of B (1.6 wt %) (inset of Figure 2a).

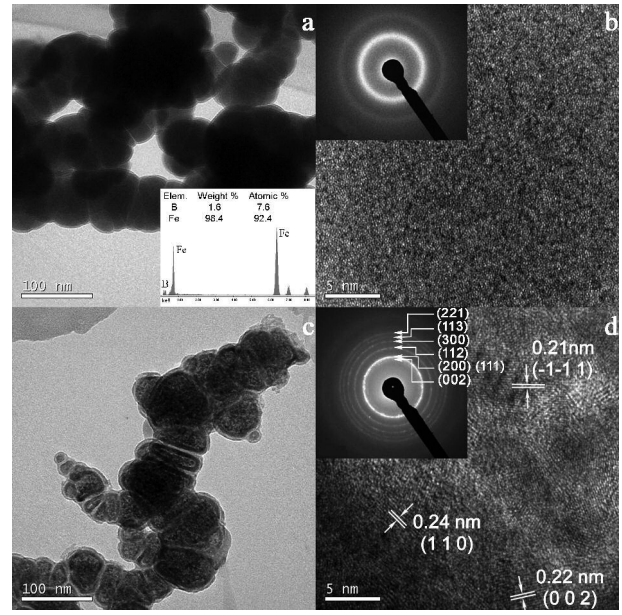

Figure 2. TEM image of the amorphous iron precursor and final product nitrided at 573 K. (a) Ball-like TEM image of the iron precursor (with EDAX result inner). (b) The short-range order (not long-range order) structure of amorphous iron (with SAED image inset). (c) TEM image of final product ϵ-$Fe_{2-3}N$. (d) Crystalline lattice structure of ϵ-$Fe_{2-3}N$ (with SAED image inset).

The amorphous iron precursor was nitrided at different temperatures. After nitridation at temperatures below 523 K (including 523 K), the final product was still amorphous iron. The elemental analysis result shows that it contains little nitrogen (0.45 wt %). The XRD pattern (Figure S1) shows that amorphous iron the product turned to α-Fe after it was annealed at 773 K under argon flow. The combined results of elemental analysis and XRD prove that nitridation could not take place at such a low temperature. When the nitriding temperature was increased to 548 K, a polycrystalline mixture consisting of mainly ϵ-$Fe_{2-3}N$, γ'-Fe_4N, and α-Fe was formed. This means that the amorphous iron begins to undergo nitridation at a temperature as low as 548 K. When the nitriding temperature was increased above 573 K, single-phase ϵ-$Fe_{2-3}N$ was obtained. Almost no peak related to γ'-Fe_4N and α-Fe in the XRD pattern was found (Figures 1 and S4). The elemental analysis shows that atomic ratio of Fe and N is 2.46. The TEM image of the product prepared at 573 K was shown in Figure 2c. The morphology of the product is still spherical, similar to that of the precursor. The result of SAED pattern proves the polycrystalline nature of the product, and the diffraction rings corresponding to different crystallographic planes are indexed in Figure 2d. The HRTEM image displays the mean crystalline grain size of the ϵ-$Fe_{2-3}N$ is around 10 nm (Figure 2d). The measured spacing values of crystal lattices are 0.21, 0.22, and 0.24 nm, which are in good agreement with the *d*-spacing values for the (−1−11), (002), and (110) crystallographic planes of ϵ-$Fe_{2-3}N$, respectively.

XPS was used to analyze the chemical environments of the product nitrided at 573 K. The XPS spectra of the sample after Ar^+ sputtering for 10 min are shown in Figure 3. The binding energies of Fe 2p3/2 and 2p1/2 corresponding to

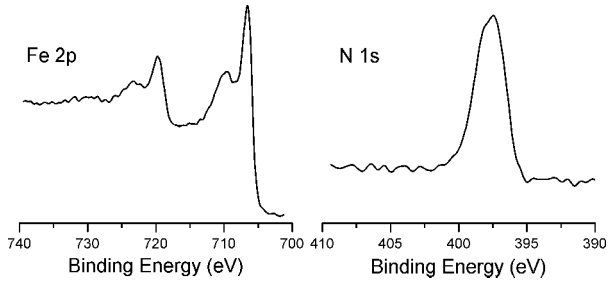

Figure 3. Fe 2p and N 1s spectra of the iron nitride sample.

iron nitride center at 706.6 and 720.0 eV. However, the small peaks of iron oxidation state (710.5 and 724.0 eV) are observed because of surface oxidation by air. The N 1s binding energy is 397.5 eV, which is characteristic of an iron nitride phase.[22,23]

The above results indicate that the nitridation of amorphous iron can occur at a low temperature of 548 K and can totally convert to ϵ-$Fe_{2-3}N$ at 573K. However, amorphous iron holds a metastable structure, and it will turn to crystalline iron when heated above its crystallization temperature. Because ϵ-phase iron nitride cannot be formed from crystalline iron at such a low temperature from thermodynamics view,[18] it is important to have precursors of nitridation in an amorphous state. It means that the amorphous precursor requires a higher crystallization temperature than the nitridation temperature. Koltpin Y. et al. reported that amorphous iron, which was synthesized by a sonochemical method, was nitrided at 673 K, and finally converted to Fe_4N.[24] The temperature was about 100 K higher than ours. It is attributed to the amorphous iron precursor they used having a low crystallization temperature.[25] At a 673 K nitridation temperature, the amorphous iron was already crystallized. The real precursor was not amorphous iron but crystalline iron, and the excess Gibbs free energy stored in the metastable structures was not used but was released through the crystallization. Differential scanning calorimetry (DSC) was used to examine the crystallization process of the amorphous iron in this work, which determined whether the reactant precursor is amorphous when the reaction occurs. As shown in Figure 4, the DSC curve of the amorphous iron sample gives an broad and diffuse exothermic peak ranging from ambient temperature to ~653 K because of relaxation, and one large exothermic transition at 725 K corresponding to the crystallization of the amorphous iron. Compared with the crystallization temperature (581 K) of amorphous iron synthesized by sonochemical method,[25] the position of the crystallization peak in this work shifts to higher temperature.

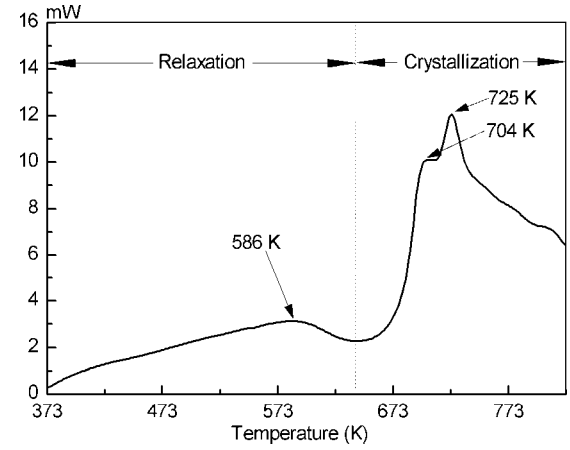

Figure 4. DSC curve of amorphous iron.

The higher crystallization temperature of our amorphous iron might be the result of the structure effect of a small amount of B in our sample, which prevents the aggregation of Fe atoms. Thus, the higher crystallization temperature makes it possible that the iron precursor keeps an amorphous state when the initial nitridation takes place. The excess Gibbs free energy stored in the amorphous structure is available to supplement to the driving force for nitridation.

To give more evidence about that nitriding iron at low temperature is attributed to the characteristic properties of the amorphous materials, the amorphous iron precursor was first annealed in argon flow for 4 h at 623 and 773 K before nitridation. As shown in XRD patterns (Figures S2a and S3a), amorphous iron was partially crystallized and completely crystallized after being annealed at 623 and 773 K, respectively. Nitridation products at 623 K consist of α-Fe and ϵ-$Fe_{2-3}N$ in the sample annealed at 623 K, and mostly α-Fe and rarely γ'-Fe_4N in the sample annealed at 773 K (Figures S2b and S3b). It confirms that the formation of ϵ-$Fe_{2-3}N$ at low temperature is because of the amorphous structure in the precursor. It also suggests that the higher the grade of crystallization of precursor is, the harder it is for nitridation to take place at low temperature.

In conclusion, we described a low-temperature approach to synthesize iron nitride using amorphous iron as the precursor. Compared with the crystallized and nanocrystalline iron, amorphous iron possesses great potential to improve the nitridation process. The reduced nitridation temperature may help to obtain mild nitridation conditions for materials.

Acknowledgment. The present work was partly supported by NSF of China (20403009) and Key Project of Chinese Ministry of Education. (105045).

Supporting Information Available: Experimental details and XRD patterns (Figures S1, S2, S3, and S4). This material is available free of charge via the Internet at http://pubs.acs.org.

IC702171S

(22) Kothari, D. C.; Nair, M. R.; Rangwala, A. A.; Lal, K. B.; Parbhawalkar, P. D.; Raole, P. M *Nucl. Instrum. Methods* **1985**, *B718*, 235.
(23) Singer, I. L.; Murday, J. S. *J. Vac. Sci. Technol.* **1980**, *17*, 327.
(24) Koltpin, Y.; Cao, X.; Prozorov, R.; Balogh, J.; Kaptas, D.; Gedanken, A. *J. Mater. Chem.* **1997**, *7*, 2453.
(25) Suslick, K. C.; Choe, S.; Cichowlas, A. A.; Grinstaff, M. W. *Nature* **1991**, *353*, 414.